ON THE CONTRIBUTION OF MOMENT-BEARING LINKS TO BENDING AND TWISTING IN A THREE-DIMENSIONAL SLIDING FILAMENT MODEL

M. HINES AND J. J. BLUM
Department of Physiology, Duke University Medical Center, Durham, North Carolina 27710

ABSTRACT Previously (Hines, M., and J. J. Blum 1983, *Biophys. J.*, 41:67–79), a method was developed that allowed one to compute curvature and twist for a three-dimensional sliding filament model. In that formalism it was difficult to specify the shear and bending moments arising from moment-bearing interfilament links such as fixed 5–6 bridges or dyneins. Euler's equation offers a straightforward method for computing these bending and shear moments when the potential energy stored in the links as a function of axonemal shape is specified. We used this approach to examine the effect of 5–6 bridges on curvature and twist for several distributions of internal shear moments. Twist changes the angle that a link makes with a doublet and thus in some circumstances may reduce the potential energy stored in those links. Twist is a second-order effect proportional to the square of the distance between an outer doublet and the neutral axis. Fixed links will not generate twist if they are symmetrically located around the axoneme.

INTRODUCTION

In a previous paper (Hines and Blum, 1983) kinematic techniques were introduced to analyze the twist and shape of an axoneme composed of filaments arranged in three dimensions (such as the 9 + 2 configuration) and constrained to move according to a sliding filament model. To solve the problem of what shape the axoneme would take under the action of an external force and any given distribution of internal shear forces between adjacent filaments, a general bending-moment equilibrium equation was introduced. Examination of this equation indicated that there were essentially only three classes of internal structures that needed to be described: the filaments themselves, which contribute a bending resistance term; pinned links that can be stretched but cannot support or transmit a bending moment (e.g., nexin links); and links that may stretch and/or carry a bending moment, such as 5–6 bridges, dynein arms when attached, and, possibly, radial bridges. In the preceding paper we derived expressions suitable for characterizing the contribution of the bending resistance of the filaments and that of pinned links to the three-dimensional shape of an axoneme. Moment-bearing links, however, resist not only stretch but also resist a change in their angle to the filament. This makes it very difficult to treat such links by directly trying to derive their contribution to the bending-moment equilibrium equation. Treatment of such links becomes much more straightforward if one considers the potential energy stored by the links as a function of shape. The effective shear terms due to this potential (which must be added to the equilibrium equation) can then be immediately derived by applying standard mechanical principles, i.e., a generalized force is the partial derivative of the potential with respect to a generalized coordinate. In this paper we develop such a formalism and use it to calculate the effect of a fixed 5–6 bridge on the shape of an axoneme with an active internal shear stress in the absence of external forces.

POTENTIAL ENERGY OF THE AXONEME

The potential energy density due to bending of the filaments in an axoneme can be written $U_b = 1/2E_{b_{ij}}k_ik_j$, where k_i are the components of the curvature in body coordinates, $E_{b_{ij}}$ are the components of the bend resistance matrix, also in body coordinates, and repeated indices are summed over the coordinates $i = 1, 2, 3$. Because the components of a bending-moment vector are

$$M_k = \frac{\partial U}{\partial k_k}, \tag{1}$$

the bending-moment components for an elastic filament are

$$M_{b_k} = -\tfrac{1}{2}(E_{b_{ik}} + E_{b_{ki}})k_i. \tag{2}$$

Thus from energy considerations, we see that the proportionality between $\mathbf{M}_b$ and $\mathbf{k}$ is necessarily a symmetric matrix; without loss of generality we define E_b to be symmetric and so obtain the usual form of the bending-moment dependence on curvature,

$$\mathbf{M}_b = -E_b\mathbf{k}. \tag{3}$$

Similarly, the shear force is obtained by differentiating the potential energy with respect to shear, i.e.,

$$S_k = -\frac{\partial U}{\partial \gamma_k}. \tag{4}$$

Here, the shear, γ, is defined via the relation $d\gamma_i/ds = k_i$ (in body coordinates) and is related to the sliding of the qth (inextensible) filament, u_q, through the relation $u_q = (\mathbf{T} \times \mathbf{L}_q) \cdot \gamma$, where $\mathbf{T}$ is the

tangent to the axoneme at arc length s and $\mathbf{L}_q$ is the vector (constant in body coordinates) in the cross section of the axoneme from the neutral axis at arc length s to the qth filament. This relation is correct to order L and neglects sliding due to twist, which is proportional to L^2 (the above is given in detail in Hines and Blum, 1983).

An example of such a potential is that due to the stretching of a pinned peripheral link connecting filaments p and $p + 1$

$$U_{p,p+1} = \frac{1}{2} E_s (|u_{p,p+1}\mathbf{T} + \mathbf{L}_{p,p+1}| - |\mathbf{L}_{p,p+1}|)^2, \quad (5)$$

where E_s is the elastic resistance of the pinned link and $\mathbf{T}$ is the unit tangent vector at arc length s. Because sliding between adjacent filaments, $u_{p,p+1}$, is independent of k_z up to third order in L, $U_{p,p+1}$ is independent of twist for all reasonable axonemal shapes. Conversely, twisting the flagellum does not store energy within pinned peripheral links.

The fundamental equilibrium equation used in the preceding paper was the derivative with respect to arc length of the moment balance equation. A shear force, S, was shown to be associated with a moment, M, via the relation $dM_i/ds = -S_i$, in body coordinates, for each component. Eqs. 1 and 4 thus provide the terms

$$-\frac{d}{ds}\left(\frac{\partial U}{\partial k_i}\right) + \frac{\partial U}{\partial \gamma_i},$$

which must be added to the equilibrium equation (Eq. 35 of Hines and Blum, 1983) to account for the effects of a structural element having a potential U.

In the present paper we wish to determine static equilibrium shapes in the absence of external forces. In this context, all the forces that determine shape are derivable from a potential. This allows the following useful reformulation of the equilibrium problem: the equilibrium shape is a shape of minimum total potential energy. Invoking this principle recasts the problem in standard variational calculus form, i.e., we wish to find the function $\gamma_i(s)$ that minimizes the total potential energy of the axoneme $\int_0^\Lambda U_T(k_i, \gamma_i, s)ds$, subject only to the ciliary boundary condition that $\gamma_i(0) = 0$. The integral is over the length of the flagellum (Λ) and U_T is the potential energy density of all structural elements. This differs from the more familiar variational problem in which both end points are fixed. It is well known that for the ciliary boundary condition problem the total potential energy is an extremum when γ is a solution to the Euler equation,

$$\frac{d}{ds}\left(\frac{\partial U_T}{\partial k_i}\right) - \frac{\partial U_T}{\partial \gamma_i} = 0 \qquad (i = 1, 2, 3), \quad (6)$$

with the boundary conditions $\gamma_i(0) = 0$ and

$$\left.\frac{\partial U_T}{\partial k_i}\right|_{s=\Lambda} = 0.$$

A simple derivation of this result is given by Gelfand and Fomin (1963), who also treat the variational problem for flagellar boundary conditions in which both ends of the axoneme are free.

Several remarks are in order at this point. First, certain important external forces, e.g., viscous forces, are derivable from a velocity-dependent potential. The variational formulation can therefore in principle be extended to include the effect of viscosity on flagellar motion. Whether this is preferable to directly deriving the viscous force terms to be inserted into the equilibrium equation is a matter of relative convenience.

Second, the choice of γ as the only independent variable describing the shape of the axoneme automatically satisfies the constraints that maintain the cross-sectional integrity of the axoneme and it is unnecessary to specify the nature of these constraints as long as their contribution to the energy stored in the axoneme does not depend on the shape of the axoneme.

Third, a solution of the Euler equation (or the equilibrium equation) is generally an extremum but not necessarily a shape of minimum potential energy. One must therefore test any solution found for stability. In the absence of external forces, however, the equilibrium equation is linear and thus has a unique solution that is necessarily the shape of minimum potential energy.

THE 5–6 BRIDGE

The procedure for adding terms to the equilibrium equation when the potential energy of a structure is known introduces a way to analyze links that can transmit bending moments. The previous treatment showed that pinned links could not generate twist in response to internal forces. However, in many cilia and flagella there is an apparently rigid 5–6 bridge whose function is unknown, but it appears to prevent appreciable sliding between outer doublets 5 and 6. To assess the effect of such moment-bearing links on the shape of a flagellum, we model the 5–6 bridge as a structure whose energy of distortion depends on the angle, ϵ, that the bridge makes with its doublets and we choose the simplest form for its potential energy,

$$U_{5,6} = E_{5,6}\epsilon^2/2, \quad (7)$$

where ϵ is measured from the normal to the doublets (Fig. 1). If one considers the 5–6 bridge to be a relatively rigid single rod connecting the two doublets, this choice of the form of $U_{5,6}$ is an approximation valid only for small γ, because it assumes that no appreciable stretching of the rod occurs. Therefore, we can only consider very stiff links that do not allow significant sliding between doublets 5 and 6.

Before using $U_{5,6}$ in the Euler equation, it must be written in terms of γ and $\mathbf{k}$. The direction of a fixed link connecting doublets 5 and 6 is (first order) given by the

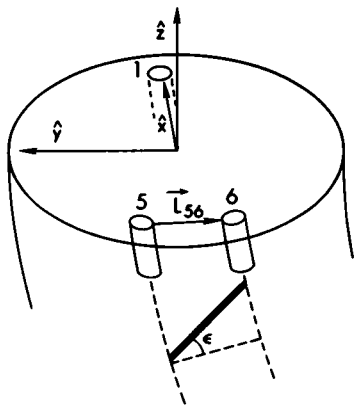

FIGURE 1 The orientation of body coordinates relative to filaments in an axoneme is shown. The unit vector $\hat{\mathbf{x}}$ points from the neutral axis to filament number 1. $L_{5,6}$ is the vector from filament 5 to filament 6 and is in the negative $\hat{\mathbf{y}}$ direction. The heavy line between filaments 5 and 6 represents a link. ϵ is the complement of the angle between this link and the tangent to filament 5 at its insertion point s.

vector $u_{5,6}\mathbf{T} + \mathbf{L}_{5,6}$, whereas the tangent vector to doublet 5 is given (also first order) by $\mathbf{T}_5 = \mathbf{T} + \mathbf{k} \times \mathbf{L}_5$. From the definition that $\epsilon = 0$ when the link and tangent are at right angles, we have

$$\sin \epsilon = (u_{5,6}\,\mathbf{T} + \mathbf{L}_{5,6}) \cdot \frac{(\mathbf{T} + \mathbf{k} \times \mathbf{L}_5)}{|u_{5,6}\,\mathbf{T} + \mathbf{L}_{5,6}||\mathbf{T} + \mathbf{k} \times \mathbf{L}_5|}. \quad (8)$$

Keeping only the lowest-order nonzero terms in Eq. 8 gives, for small ϵ:

$$\epsilon = \frac{u_{5,6} + \mathbf{L}_{5,6} \cdot (\mathbf{k} \times \mathbf{L}_5)}{(u_{5,6}^2 + L_{5,6}^2)^{1/2}}. \quad (9)$$

It is convenient to choose the body coordinate system so that the vector from doublet 5 to doublet 6 is in the $-y$ direction (see Fig. 1). Then, because $u_{5,6} = (\mathbf{T} \times \mathbf{L}_{5,6}) \cdot \boldsymbol{\gamma}$ and $\mathbf{k} \cdot (\mathbf{L}_5 \times \mathbf{L}_{5,6})/L_{5,6} = Lk_z \sin 70°$, where L is the radial distance of the outer doublets from the central axis, Eq. 9 becomes (because $\sin 70° \approx 1$):

$$\epsilon = \frac{\gamma_x + Lk_z}{(1 + \gamma_x)^{1/2}}. \quad (10)$$

For $\gamma_x \ll 1$,

$$\epsilon = \gamma_x + Lk_z. \quad (11)$$

The contributions of sliding and twisting to axonemal distortion are shown in Fig. 2. To within the limits of accuracy imposed by these approximations, the effective shear force (cf. Eq. 4) developed in response to a small relative sliding between doublets 5 and 6 is then

$$\mathbf{S}_{5,6} = -E_{5,6}(\gamma_x + Lk_z)\hat{\mathbf{x}}, \quad (12)$$

and the moment developed by this fixed bridge is (cf. Eq. 1)

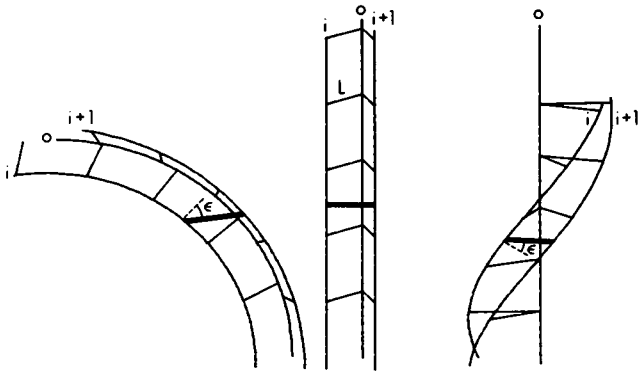

FIGURE 2 Examples of link distortion caused by sliding and twisting are shown. The middle panel shows an undistorted link between filaments i and $i + 1$. The left panel shows that sliding causes a change in angle, ϵ, between the link and the ith filament corresponding to the amount of sliding, γ_x. The right panel shows that pure twist, although it does not produce relative sliding, changes the angle between the link and the ith filament; the change in ϵ is equal to Lk_z, where L is the distance between the filament and the neutral axis, designated by 0.

$$\mathbf{M}_{5,6} = -LE_{5,6}(\gamma_x + Lk_z)\hat{\mathbf{z}}, \quad (13)$$

which is a pure twisting moment. It is this term that couples shear strain in a moment-bearing link to twist.

Before investigating this case further, it is instructive to calculate $\mathbf{S}$ and $\mathbf{M}$ in the presence of an additional set of similarly rigid links located between doublets 1 and 2. In that case the vector from doublet 1 to doublet 2 is approximately in the $+y$ direction (see Fig. 1) and $\mathbf{L}_1$ is in the $+x$ direction, so $\epsilon = -\gamma_x + Lk_z$ and

$$U_{5,6} + U_{1,2} = E_{5,6}(\gamma_x^2 + L^2k_z^2). \quad (14)$$

Then the shear force is

$$\mathbf{S}_{5,6} + \mathbf{S}_{1,2} = -2E_{5,6}\gamma_x\hat{\mathbf{x}}, \quad (15)$$

and the twisting moment is

$$\mathbf{M}_{5,6} + \mathbf{M}_{1,2} = -2L^2E_{5,6}k_z\hat{\mathbf{z}}. \quad (16)$$

A twisting moment now arises only if a twist of magnitude k_z is imposed on the axoneme, i.e., internal shear forces no longer cause net twists. The presence of moment-bearing links between doublets 5 and 6 and between doublets 1 and 2 almost completely[1] converts the behavior of the system to that of an axoneme with pinned links and a slightly increased twist resistance. Thus the coupling of shear strain to twist is dependent on the asymmetrical placement of peripheral moment-bearing links around the axoneme.

STIFFNESS OF 5–6 BRIDGE

Before computing the bending and twisting due to an internal shear force, it is necessary to make an order of magnitude estimate for the value of $E_{5,6}$. If we consider the bridge to be firmly tied to the doublet, then the bridge will be deformed into an s shape because doublet 5 slides relative to doublet 6, with the points of insertion remaining at right angles. Recalling the definition of ϵ as the deviation from a right angle that the bridge makes with the 5–6 doublets, we locate ϵ and the direction of the tangent to the bridge at the midpoint of the bridge, where the distortion is greatest. For a rigid rod of length R with bend resistance EI acted on by external forces, ϕ, moment equilibrium requires that $EI(\mathrm{d}^2\alpha/\mathrm{d}x^2) + F_{\text{ext}} = 0$, where $(\mathrm{d}F_{\text{ext}}/\mathrm{d}x) = \phi$. In the absence of external forces, therefore $\mathrm{d}^3\alpha/\mathrm{d}x^3 = 0$ and $\alpha = 4x(R - x)\epsilon/R^2$. Of course the approximation must hold that sliding is small enough so that the bridge does not lengthen significantly. The curvature is then given by

$$k = \frac{\mathrm{d}\alpha}{\mathrm{d}x} = \frac{4\epsilon(R - 2x)}{R^2}. \quad (17)$$

[1]To be exact, fixed links between doublets 1 and 2 and 5 and 6 are not completely opposite one another, but make an angle of 160°. This leads to a cancellation of only 65% of the shear dependence of the twisting moment instead of the 100% if the 5,6 and 1,2 doublets were exactly opposite.

The energy of distortion of the bridge is

$$U = \frac{EI}{2}\int_0^R k^2 dx = \frac{1}{2}\left(\frac{16EI}{3R}\right)\epsilon^2. \quad (18)$$

The energy density per unit arc length contributed by the 5–6 bridges is then (cf. Eq. 11)

$$U_{5,6} = \frac{16}{6dL_{5,6}} EI(\gamma_x + Lk_z)^2, \quad (19)$$

where d is the separation between adjacent 5–6 bridges. Comparison of Eq. 19 with Eq. 7 shows that

$$E_{5,6} = \frac{16EI}{3dL_{5,6}}. \quad (20)$$

The moment of inertia, I, of a rigid rod of radius r is $I = \pi r^4/2$. Taking r = 10 nm, $E = 10^7$ pN/μm^2 (Hines and Blum, 1983), d = 24 nm, and $L_{5,6}$ (the bridge length) = 40 nm, then $E_{5,6} \approx 10^3$pN.

An alternative calculation is based on an analogy of the 5–6 bridge to a dynein arm in rigor. Hines and Blum (1979) estimated that a reasonable value for the force generated by an attached dynein arm is 1.6 pN/nm · $(x - x_0)$, where $x - x_0$ is a measure of dynein arm displacement. The energy of distortion per dynein is then 0.8 pN/nm · $(x - x_0)^2$. Replacing $x - x_0$ by $L_{5,6}\epsilon$ and assuming that bridges are separated by 24 nm, one obtains $E_{5,6} \approx 100$ pN. Thus $E_{5,6}$ is likely to range between 10^2 and 10^3 pN. From Eq. 16 these two estimates imply that the effect of two symmetrically located moment-bearing links would increase the twist resistance of an axoneme from ~2 to 20 pN μm^2. According to the discussion in Hines and Blum (1983), a reasonable estimate of the bend resistance of a single doublet is ~10 pN μm^2, which may be identified with component E_{yy} of the bend resistance matrix. Because the twist resistance, E_{zz}, is 4.5-fold larger than E_{yy}, E_{zz} for an axoneme without moment-bearing links is ~45 per doublet for a total of ~450 pN μm^2. Thus symmetrically placed moment-bearing links will contribute little to the twist resistance.

COMPUTER SIMULATIONS OF FLAGELLAR SHAPE

Computer simulations of the effect of the 5–6 bridge on the twist of an axoneme were carried out using the computer program described in Hines and Blum (1983) with the terms $E_{5,6}(\gamma_x + Lk_z)$ and $-(d/ds)LE_{5,6}(\gamma_x + Lk_z)$ added to the x and z components of the equilibrium equation (Eq. 35 of that paper). The distal boundary condition was modified to reflect the contribution of the 5–6 bridge to the twisting moment according to Eq. 13. No external forces were applied and bending was caused solely by an explicit specification of active force, $\mathbf{S}_D$ (derived from a potential, $U_D = -S_{D_i}\gamma_i$). In the absence of external force the equations are linear so no iterations are necessary.

In Figs. 3–10, unless otherwise specified, the following values are used: axonemal length = 40 μm (divided for purposes of computation into 30 segments), L = 100 nm, and E_s = 0 pN. The magnitude of $E_{b_{zz}}$ was reduced in these computations to make the otherwise small twisting effects readily apparent. The active shear force is assumed to be uniformly distributed along the length of the axonemes unless otherwise stated. In Figs. 3–5, k_y is zero at all s values because $S_{D_y} = 0$ for these simulations.

Fig. 3 shows the effect of varying the internal shear force, S_{D_x}, from 25 to 100 pN. This shear force, uniformly distributed along the entire axoneme, tends to cause sliding between doublets 5 and 6 and thereby generates a local bend in the proximal portion of the axoneme (sliding is not allowed at the proximal end). Because γ is constant in the distal portion, the rate of twist is also constant. Therefore both bend angle and twist are proportional to the active shear force.

The dependence of twist on the value of $E_{5,6}$ is more subtle and is displayed in Fig. 4 for an axoneme with fourfold higher values for $E_{b_{xx}}$ and $E_{b_{yy}}$ and a 10-fold lower twist resistance than for the axoneme shown in Fig. 3. The left panel shows that for sufficiently low values of $E_{5,6}$, twist vanishes as expected because M_z is proportional to $E_{5,6}$ and γ_x approaches a limiting value determined only by the bending resistance of the filaments (Eq. 3). As $E_{5,6}$ increases, its shear resistance dominates the bending resistance in balancing the (constant) active shear force. Thus $E_{5,6}\ \gamma_x$ remains constant over a wide range of $E_{5,6}$ values and therefore M_z becomes constant over most of the length of the axoneme. At extremely large values of $E_{5,6}$ the twist resistance term $L^2E_{5,6}$ in Eq. 13 becomes dominant and k_z goes to zero. The right panel in Fig. 4 further illustrates these effects by displaying the amount of twisting and of sliding at the distal end as a function of $E_{5,6}$.

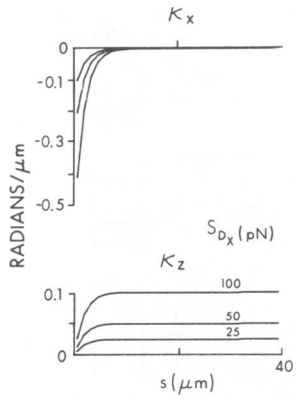

FIGURE 3 The effect of active shear force on components of the curvature vector is demonstrated. Active shear moments (per unit length), of magnitude 25, 50, and 100 pN, are applied uniformly (in the $\hat{x}$ direction) along the length of the axoneme. The 5–6 bridge is stiff enough to confine bending to the proximal end of the axoneme. Parameter values are $E_{5,6}$ = 100 pN; $E_{b_{xx}} = E_{b_{yy}}$ = 500 pN μm^2; $E_{b_{zz}}$ = 100 pN μm^2; and S_{D_x} = 25, 50, and 100 pN as shown.

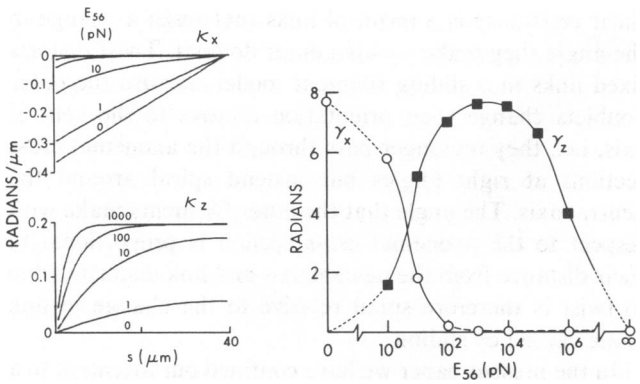

FIGURE 4 Effect of $E_{5,6}$ on bending and twist under uniform shear moment per unit length is demonstrated. The magnitude of $E_{5,6}$ varies as shown. The left panels show the components of the curvature vector along the axoneme. The right panel shows the cumulative sliding (γ_x) and twist (γ_z) at the distal end of the axoneme ($s = 40$ μm) as a function of $E_{5,6}$. Parameter values are $E_{b_{xx}} = E_{b_{yy}} = 2{,}000$ pN μm^2; $E_{b_{zz}} = 10$ pN μm^2; and $S_{D_x} = 20$ pN.

Fig. 5 shows a stereoscopic view of flagellar shape for $E_{5,6} = 1{,}000$ pN. The combination of a uniform active shear force and a very stiff 5–6 bridge causes an essentially pure uniform twist. If to this axoneme one now adds a small additional active shear force in the y direction ($S_{D_y} = 1$ pN), it now develops curvature in the y direction that decreases uniformly from the proximal to the distal end (Fig. 6). If the 5,6 bridges are treated as pinned links then, of course, no twisting occurs (see the upper pair of stereoscopic views in Fig. 6).

The effect of having two opposite and equal local shear forces in an axoneme with stiff 5,6 bridges and pinned (nexin) links is shown in Fig. 7. Maximum twisting curvature, k_z, occurs at the center of each active region and

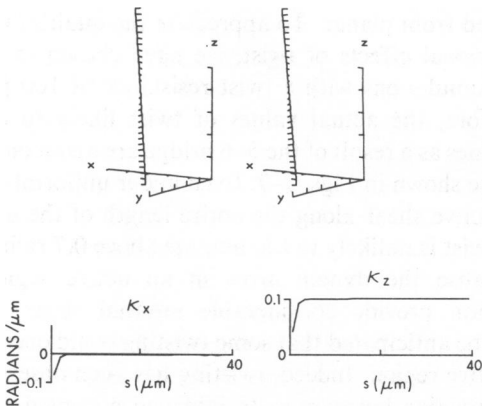

FIGURE 5 The pattern of twist in an axoneme with a very stiff $E_{5,6}$ bridge and uniform active force are demonstrated. The right panel of this figure shows a stereoscopic view of the axoneme. Bending is small ($\gamma_x = 0.1$ radians at the distal end) and localized at the proximal end whereas twisting is uniform along the axonemal length, reaching a value of 3.9 radians at the distal end. Parameter values are $E_{5,6} = 1{,}000$ pN; $E_{b_{xx}}$, $E_{b_{yy}}$, $E_{b_{zz}} = 500$, 300, 100 pN μm^2, respectively; and $S_{D_x} = 100$ pN.

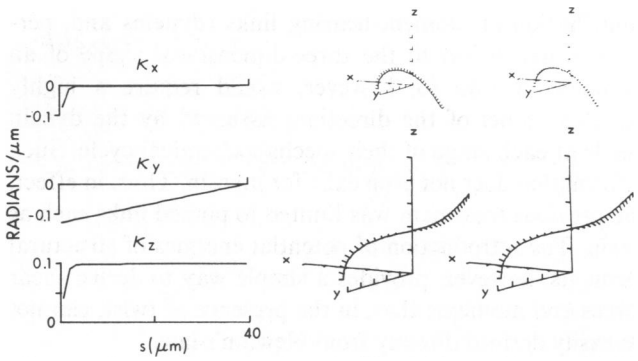

FIGURE 6 The bending and twisting in an axoneme with the active shear forces in the x and y direction are demonstrated. The left shows the variation of k_x, k_y, and k_z along the axoneme, and the lower right panel shows a stereoscopic view of the axoneme. Parameter values are $E_{5,6} = 1{,}000$ pN; $E_{b_{xx}}$, $E_{b_{yy}}$, $E_{b_{zz}} = 500$, 300, 100 pN μm^2, respectively; $S_{D_x} = 100$; pN; and $S_{D_y} = 1$ pN. The upper right panel shows the effect of treating the 5,6 bridges as pinned links with a shear resistance of 1,000 pN.

vanishes rapidly where there is no active shear force. The two regions of k_z, however, have opposite signs so the distal end of the axoneme has no twist. k_y differs at the proximal and distal ends because the boundary condition at the distal end is that $k_y = 0$, whereas at the proximal end the filaments are tied together and $\gamma_y = 0$.

DISCUSSION

In a preceding paper (Hines and Blum, 1983) we derived expressions that could, in principle, be used to describe the

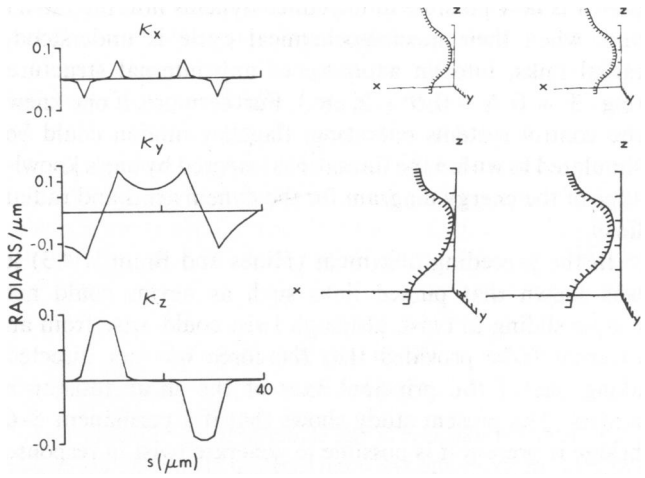

FIGURE 7 The bending and twisting in an axoneme with stiff 5,6 bridges, pinned links between adjacent filaments, and equal and opposite active shear forces in segments 5–9 and 20–24 is shown. The active shear force in segments 5–9 is $S_{D_x} = 100$ pN and $S_{D_y} = 20$ pN; and in segments 20–24 is $S_{D_x} = -100$ and $S_{D_y} = -20$ pN. The parameters are $E_{56} = 1{,}000$ pN, $E_{s_x} = E_{s_y} = 10$ pN, and $E_{b_{xx}}$, $E_{b_{yy}}$, $E_{b_{zz}} = 500$, 300, 100 pN μm^2, respectively. The left panels show the components of the curvature vector along the axoneme. The lower right panels show a stereoscopic view of the shape of the axoneme. The upper stereoscopic view shows the effect of replacing the 5,6 bridges by pinned links, i.e., $E_{56} = 0$, $E_{s_x} = 1{,}010$ pN and $E_{s_y} = 10$ pN.

contribution of moment-bearing links (dyneins and, perhaps, radial links) to the three-dimensional shape of an axoneme. To do so, however, would require a highly detailed model of the directions assumed by the dynein heads at each stage of their mechanochemical cycle. Such information does not even exist for myosin. Thus, in effect, the previous treatment was limited to pinned links such as nexin. The introduction of potential energies of structural elements, however, provides a simple way to derive shear forces and moments that, in the presence of twist, can not be easily derived directly from Newton's law.

Reformulation of the static equilibrium problem in terms of an energy minimization principle has several advantages. First, it is an elegant validation of the form of the equilibrium equation (i.e., derivative of the moment balance equation) that we have been using. Second, the variational formulation does not require any assumptions concerning the forces of constraint. Indeed, that concept no longer appears and, instead, the geometrical constraints (such as that the axoneme retain its internal geometry) are taken care of by an appropriate choice of generalized coordinates. Third, the most convenient way to specify the dynein mechanochemical cycle is in terms of an energy vs. distance diagram (Hill, 1974), as introduced by Brokaw (1975) for studies of flagellar motility in a two-dimensional model. In the present paper we have used the Euler equation to investigate the effect of a fixed 5–6 bridge on the bending and twisting pattern in axonemes with internal point forces rather than with dyneins undergoing a specified mechanochemical cycle. It should be clear, however, that it is now possible to introduce dyneins into the model and, when their mechanochemical cycle is understood, radial links, into an axoneme of any internal structure (e.g., 3 + 0, 6 + 0, 9 + 2, etc.). Furthermore, if one knew the control systems operating, flagellar motion could be simulated to within the limitations imposed by one's knowledge of the energy diagram for the dynein arms and radial links.

In the preceding treatment (Hines and Blum, 1983) it was shown that pinned links such as nexins could not couple sliding to twist, although twist could arise from an external force provided that the force was not directed along one of the principal axes of the shear resistance matrix. The present study shows that if a permanent 5–6 bridge is present it is possible to generate twist in response to internal shear forces. However, because the coupling between link deformation and twist is proportional to the radius of the axoneme, relatively large shear forces are required to generate appreciable twist. This accords well with findings (Omoto and Brokaw, 1983) that the twist that is observed in demembranated sperm tail axonemes is almost entirely a result of external forces caused by interaction of the axoneme with the substrate on which the axoneme lies.

Although internal shear forces will not cause twist in an axoneme with pinned links only, twist does arise when shear resistance is a result of links that resist a change in the angle they make with an outer doublet. Twist distorts fixed links in a sliding filament model because the outer doublets change their orientation relative to the neutral axis, i.e., they no longer pass through the axonemal cross sections at right angles but instead spiral around the neutral axis. The angle that the outer filaments make with respect to the axonemal cross section is proportional to their distance from the neutral axis and link distortion due to twist is therefore small relative to the change in link angle caused by sliding.

In the present paper we have confined our attention to a particular set of stiff links, the 5–6 bridges that occur in a number of axonemes. These bridges are essentially parallel to a line drawn between the two single tubules of the central pair and thus tend to define the plane of bending in conjunction with the extra stiffness in one direction due to the central pair. Twisting curvature occurs in regions where there is active moment tending to shear the 5–6 bridge (Fig. 7). Insight into the factors governing the magnitude of the twist come from the following qualitative considerations. The amount of twist, k_z, is proportional to the twisting moment, M_z, generated by the 5–6 bridge and inversely proportional to the twisting resistance, $E_{b_{zz}}$. M_z, in turn, is proportional to the shear, γ_x, of the 5–6 bridge, which is determined from a combination of axonemal bend resistance, $E_{b_{xx}}$, 5–6 bridge stiffness, $E_{5,6}$, and the magnitude of the active shear force in the direction tending to shear the 5–6 bridge.

In the previous paper it was shown that a slender filament has a bending resistance to twisting resistance ratio of ~3:5. For an $E_{b_{xx}}$ value of 500 pN μm^2 used in the current simulations, the expected value of $E_{b_{zz}}$ would be ~800 pN μm^2. If this value of $E_{b_{zz}}$ had been used, the twist observed in Figs. 3–7 would have been reduced by a factor of 8 and therefore ciliary shapes would have scarcely deviated from planar. To appreciate the qualitative three-dimensional effects of twist, we have chosen to perform these simulations with a twist resistance of 100 pN μm^2. Therefore, the actual values of twist likely to occur in axonemes as a result of the 5–6 bridge are about one-eighth of those shown in Figs. 3–7. Even under uniformly distributed active shear along the entire length of the axoneme, total twist is unlikely to accumulate above 0.7 radians.

Because the dynein arms in an active region of a flagellum provide considerable internal shear force, it might be anticipated that some twisting could occur within the active region. Indeed, twisting has been observed near each junction between a straight and a curved region in rigor wave sea urchin sperm tails (Gibbons, 1975). Of particular interest is the observation that twist put in at one end of a straight region is unwound at the other end, so that little or no twist accumulates over the whole length of the axoneme. This is precisely the qualitative behavior observed in Fig. 7 for an axoneme with 5–6 bridges having opposite and equal local shear forces at two separate

regions. Quantitative considerations, however, must wait until the present analysis is extended to the case of detachable dynein arms (Hines, M., and J. J. Blum, manuscript submitted for publication).

This work was supported by National Institutes of Health grant NS 11613.

Received for publication 12 August 1983 and in final form 13 March 1984.

REFERENCES

Brokaw, C. J. 1975. Molecular mechanism for oscillation in flagella and muscle. *Proc. Natl. Acad. Sci. USA.* 72:3102–3106.

Gelfand, I. M., and S. V. Fomin. 1963. Calculus of variations Section 6. A simple variable end point problem. Prentice-Hall, Inc., Englewood Cliffs, New Jersey. 25–27.

Gibbons, I. R. 1975. The molecular basis of flagellar motility in sea urchin spermatozoa. *In* Molecules and Cell Movement. S. Inoue and R. E. Stephens, editors. Raven Press, New York. 207–231.

Hill, T. L. 1974. Theoretical formalism for the sliding filament model of contraction of striated muscle. Part I. *Prog. Biophys. Mol. Biol.* 28:267–340.

Hines, M., and J. J. Blum. 1979. Bend propagation in flagella. II. Incorporation of dynein cross-bridge kinetics into the equations of motion. *Biophys. J.* 25:421–442.

Hines, M., and J. J. Blum. 1983. Three-dimensional mechanics of eukaryotic flagella. *Biophys. J.* 41:67–79.

Omoto, C. J., and C. J. Brokaw. 1983. Quantitative analysis of axonemal bends and twists in the quiescent state of *Ciona* sperm flagella. *Cell Motil.* 3:247–259.